

The Eurasia Proceedings of Science, Technology, Engineering and Mathematics (EPSTEM), 2025

Volume 38, Pages 316-322

**IConTES 2025: International Conference on Technology, Engineering and Science**

## Effects of Elastic Deformation on the Corrosion of 316l in 3.5% NaCl

**Allou Djilali**

Research Center in Industrial Technologies

**Amraoui Rachid**

Research Center in Industrial Technologies

**Djemmah Sarra**

University of Mons

**Benmohamed Manel**

Research Center in Industrial Technologies

**Younes Abderahman**

Research Center in Industrial Technologies

**Abada Abderahim**

University of Saad Dahlab Blida 1

**Abstract:** 316L is an austenitic stainless steel widely used in BOPs (Blowout Preventers) due to its exceptional properties of corrosion resistance, toughness and mechanical strength in extreme environments. In this study, we will investigate the impact of elastic deformation on the hardening properties and electrochemical behavior of 316L steel in 3.5% NaCl. The results indicate that 316L stainless steel is sensitive to work hardening. In the unstressed state, it has a crystalline structure with randomly distributed dislocations and a hardness of 234 HV10 at the yield point (Re). When hardness reaches its peak (240 HV10), the material reaches the threshold where dislocations can move irreversibly. Dislocation density is then at its maximum in the elastic regime, and the material enters the plastic range. Electrochemical tests carried out on 316L stainless steel under various mechanical stresses show a contrasting influence of stress on corrosion behavior. While the unstressed sample shows a corrosion current density ( $I_{corr}$ ) of 2.69  $\mu$ A, this value drops to 1.25  $\mu$ A for a sample stressed to 75% of yield strength (Re), indicating improved corrosion resistance. This improvement can be attributed to densification or partial repair of the passive film under moderate mechanical stress. These results underline the importance of carefully controlling the level of mechanical stress to simultaneously optimize mechanical properties and durability in a corrosive environment.

**Keywords:** 316L, Yield strength (Re), Hardness HV10, Corrosion, Mechanical stress

## Introduction

Austenitic stainless steel 316L is widely used in demanding corrosive environments on account of high corrosion resistance along with superb mechanical properties (Sedriks 1996, Marcus 1998, Revie et al. 2008, and Allou et al. 2020). These characteristics make it into a material for choice in biomedical, chemical, nuclear, and offshore industries (Allou et al. 2021, Benafia et al. 2018). Mechanical stress and aggressive media frequently affect components there (Olsson et al. 1995. Marcus 2011). Researchers have studied the

- This is an Open Access article distributed under the terms of the Creative Commons Attribution-Noncommercial 4.0 Unported License, permitting all non-commercial use, distribution, and reproduction in any medium, provided the original work is properly cited.

- Selection and peer-review under responsibility of the Organizing Committee of the Conference

electrochemical behavior of 316L extensively though mechanical loading within the elastic regime relatively underexplores its specific influence on corrosion response (Zhang et al. Krohn, et al. 2021, Yun et al 2024).

In this study, 316L stainless steel was subjected to a set of varying levels of mechanical stress ranging from 0 % to 100 % of the yield strength (Re) because it remained within the elastic domain, so as to assess the impact on general corrosion behavior. Electrochemical parameters characterized the passive behavior for the alloy (Gaoxiang et al. 2019). Corrosion rate (mm/year), corrosion current density (Icorr), as well as corrosion potential (Ecorr) were among parameters that were measured. Concurrently, Vickers hardness (HV10) was evaluated. Applied stress induced mechanical effects were the goal to monitor (Frankel.2003, Tabor 2000, Cihal et al. 2019, Djemmah, et al 2023).

The results revealed that there was a non-linear trend: slight anodic activation occurred at low stress levels (25 % Re), then passivation improved greatly at 75 to 100 % Re. The hardness increases correlates to this evolution, so this correlation implies a good interaction between passive film reinforcement and mechanical hardening (Ouadah et al 2018, Macdonald 2011, Djemmah et al 2024). These results present helpful perceptions and greater comprehension of mechanical-electrochemical interaction within stainless steels for designing components subjected to combined chemical and mechanical stresses.

## Materials and Method

The chemical composition of the 316L stainless steels sample was obtained by means of a spectrophotometer XRF S8 Tiger-Bruker spectroscopy equipment is given in Table 1. steels had a rectangular shape 25.5x 13 mm with thicknesses (5.06 mm)

Table 1. Chemical composition of 316L (wt.%)

Alloy	C	Si	Mn	Cr	Mo	Ni	Cu	Ti	P	S	Fe
316L	0.03	0.52	1.09	17.23	1.97	10.91	0.15	0.18	0.04	0.01	all

Tensile tests were conducted on four specimens to evaluate the mechanical behavior of 316L stainless steel within the elastic domain, using an INSTRON testing machine with a 100 N load capacity. Fig. 1 shows the specimens after tensile testing. A reference specimen was subjected to a full tensile test up to fracture in order to determine the elastic limit (Re). Three additional specimens. A (25% of Re), B (75% of Re), and C (100% of Re) were tested up to their respective stress levels. For specimens A, B, and C, once the target stress level was reached, the test was paused while maintaining the applied load for 2 hours. After this holding period, the specimens were removed and sectioned at mid-length for further analysis. All samples were prepared and embedded in an epoxy resin, with an electric contact for using them as working electrode in a standard three-electrode cell. The other electrodes were a Pt counter electrode and a SCE reference electrode. The exposed surfaces of the working electrodes were 25.5 x 0.5 cm<sup>2</sup>. Electrochemical tests were performed at room temperature ( 20 to 25 °C). The electrochemical impedance spectroscopy (EIS) and potentiodynamic polarization curve measurements were conducted using the PGSTAT302N potentiostat and Autolab electrochemical analyzer instruments from Metrohm, with NOVA software. The potentiodynamic polarization curve was measured with a sweep rate of 0.01 V/s. This curve provides information about the corrosion behavior and allows for the determination of corrosion current and potential. EIS measurements were performed in a frequency range of 100 kHz to 100 MHz, with an amplitude of 0.01 V.

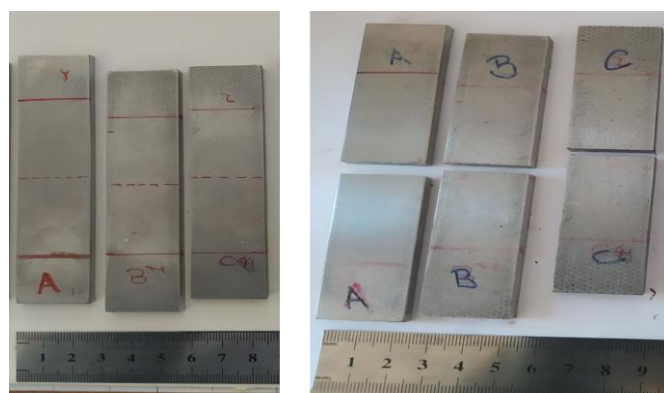


Figure 1. Tensile specimens after testing, before and after sectioning.

## Results and Discussion

### Effect of Stress Variation on Hardness

Figure 1 shows the stress-strain curve with interruptions at three distinct points: A at 25% of the yield strength (Re), B at 75% of Re, and C at Re.

Table 2. Variation of applied load, as well as the change in cross-section of each sample

Position in traction curve	Load value (Mpa)	L x Th
Tensile test piece	00	25.5x5.06 =129.03
A	25% of Re	25.4 x 5.06 =128.52
B	75% of Re	25.27 x 5.06=127.87
C (Re)	100% of Re	25.19 x 5.03 =126.71

We can observe that as the applied stress increases, there is a measurable, albeit small, reduction in the cross-sectional area of the specimen, this trend is clearly illustrated in Figure 2. The tensile specimen initially had central dimensions of 25.5 mm  $\times$  5.06 mm, corresponding to a cross-sectional area of 129.03 mm<sup>2</sup>. As deformation progressed, a slight decrease in area was recorded, reaching 126.71 mm<sup>2</sup> at point C (corresponding to the yield strength, Re).

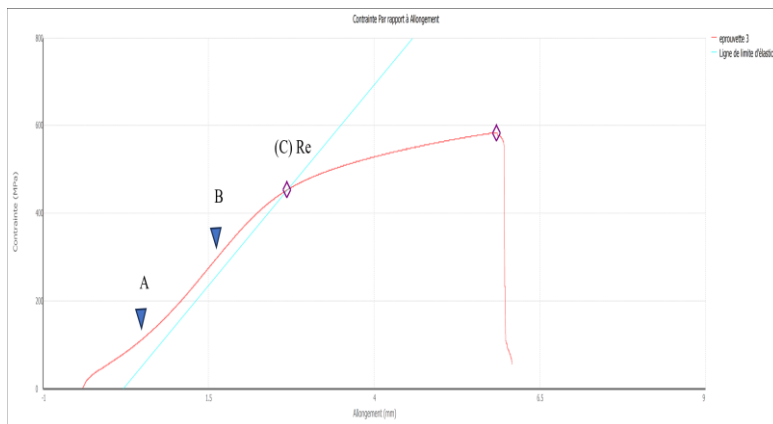


Figure 2. Tensile test graph for specimen 316 L.

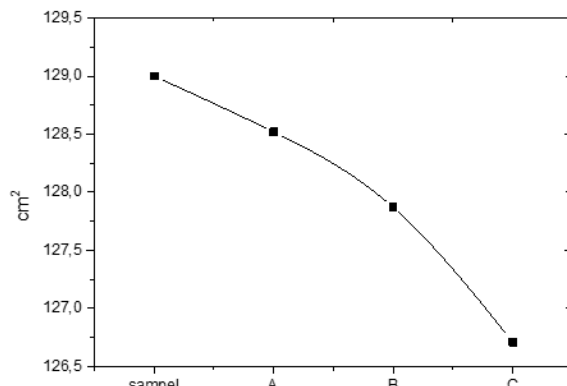


Figure 3. Surface of the specimens at the center of the tensile-tested samples in the elastic deformation range.

Figure 4. illustrates the evolution of hardness, based on the values reported in Table 3. In the unstressed state, the hardness of 316L stainless steel is 213 HV10. As the applied stress increases, the hardness rises progressively, reaching a maximum value of 240 HV10 at the elastic limit (point C = Re), passing through 234 HV10 at point A (25% of Re) and 237 HV10 at point B (75% of Re).

In its unstressed state, the material has a crystalline structure with dislocations randomly distributed throughout the lattice. The initial hardness reflects the intrinsic resistance of the material to dislocation motion. When a stress is applied but remains within the elastic domain dislocations begin to move and gradually accumulate around obstacles such as grain boundaries, precipitates, and other dislocations. These localized micro-strains can

lead to a slight increase in dislocation density due to elastic strain hardening, even before yielding occurs. This explains the increase in hardness from 234 HV10 at 25% Re to 240 HV10 at Re.

This progression reflects the increasing internal resistance due to growing dislocation interactions. At the yield strength (Re), where the material reaches the threshold for irreversible dislocation motion, the dislocation density attains its maximum for the elastic regime, accounting for the observed peak in hardness.

Table 3. Hardness HV10 values of different test bars

	Hardness
Without stress	213
A	234
B	237
C	240

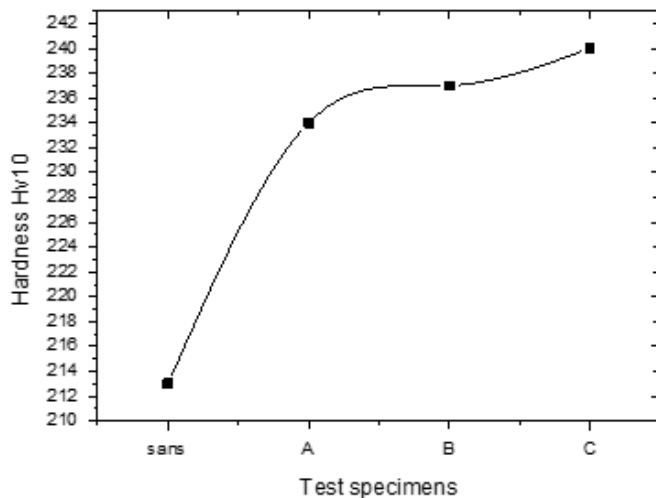


Figure 4. Hardness HV10 of different test bars

#### Effect of Stress Variation on Corrosion

Figure 5 shows the superposition of the polarization curves of the specimens (unstressed and with mechanical stresses A, B and C approaching yield strength Re) in an NaCl-based electrolyte (3.5%). They correspond to a scanning interval between -1 and 0.1 V. Ag / AgCl reference electrodes for the substrate and the sample interface, and between -0.6 and 0.4 V. Ag / AgCl reference electrode AgCl for recharging. We used the slew rate of 1 mV/s from cathode to anode direction. The results of the polarization curve of Figure 3. are summarized in Table 3. showing the corrosion potential ( $E_{corr}$ ), the corrosion current density ( $i_{corr}$ ) and the corrosion rate.

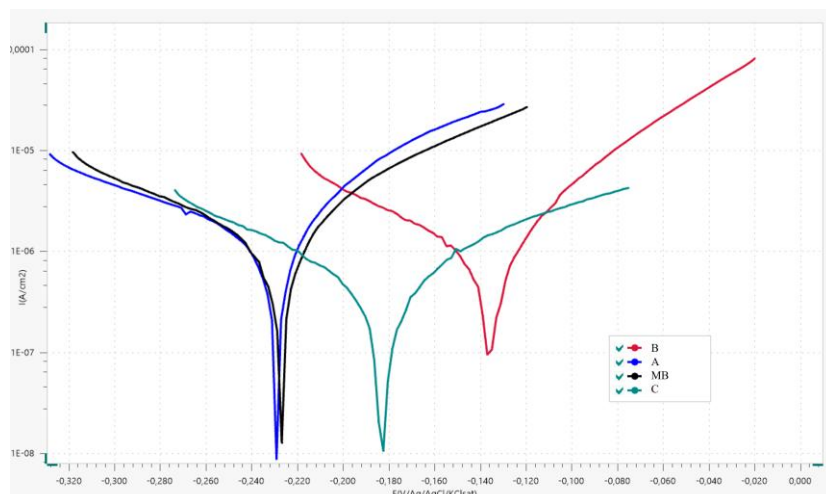


Figure 5. Polarization curves of 316L in 3.5 % of NaCl electrolyte

Table 4. Electrochemical parameters of potentiodynamic tests

	316L, without constraint	A	B	C (Re)
$E_{corr}$ (mV)	-227	-229	-136	-183
$I_{corr}$ ( $\mu$ A/cm <sup>2</sup> )	2.69	3.42	1.25	0.97
Corrosion rate(mm/year)	0.030	0.031	0.011	0.010

When the material is in its unstressed state and moves to state A, which is 25% of the Re, the corrosion potential ( $E_{corr}$ ) stays the same, between -227 and -229 mV. At this moderate stress level, which is 25% of the yield strength, the electrochemical activity of 316L isn't greatly affected. The passive layer stays intact, meaning the material continues to be protected by its passive film. However, the corrosion current ( $I_{corr}$ ) goes up from 2.69 to 3.42  $\mu$ A/cm<sup>2</sup>.

Even with low stress, there is a small increase in corrosion. This shows that the passive film is starting to be affected in small areas like through micro-cracks, defects, or dislocations that let ions move more easily. This is to be expected because mechanical stress can weaken the passive layer. The corrosion rate also increases a little, from 0.030 to 0.031 mm/year, which is a small but real change of +3.3%. This confirms that the initial mechanical stress is beginning to slightly affect the passive film's stability. Even so, the increase is still low, which means 316L still has good passivity.  $E_{corr}$  rises dramatically (from -229 to -136 mV).

From state A to state B (25% to 75% of Re). It may seem counterintuitive, but the corrosion potential significantly improves. A more noble potential could be produced by local atomic rearrangement brought on by mild plastic deformation, which would encourage the development of a denser or more stable passive film.  $I_{corr}$  rapidly decreases from 3.42 to 1.25  $\mu$ A/cm<sup>2</sup>. This implies that a more protective passive layer, probably enriched in chromium, may have been reorganized more easily as a result of deformation. Additionally, the corrosion rate drops by almost 65%, from 0.031 to 0.011 mm/year. This closely resembles the decline in  $I_{corr}$ , suggesting that the material experiences repassivation or passive film stabilization, most likely as a result of either closure or chromium oxide ( $CrO_3$ ) enrichment of the film.

When moving from state B to state C (75% to 100% of Re), the corrosion potential ( $E_{corr}$ ) drops again, going from -136 to -183 mV. As stress increases, the passive layer starts to break down, forming small cracks and defects on the surface that help corrosion happen. However, the corrosion current ( $I_{corr}$ ) keeps going down, from 1.25 to 0.97  $\mu$ A/cm<sup>2</sup>. At this point, the passive layer seems to be more stable or even stronger. This might be because stress causes a lot of defects in the material, and adding more stress doesn't create much more damage. The corrosion rate also slightly decreases, from 0.011 to 0.010 mm/year. Although the trend is still downward, the improvement is small, only about 9%. This shows that the electrochemical reactions have reached their limit, and the system is as stable as it can be. Any more stress, as long as it stays within the elastic range, won't make much difference in terms of risk or benefit.

## Conclusion

The impact of deformation in the elastic domain on the hardening properties and electrochemical behavior of 316L steel in 3.5% NaCl is assessed. The following conclusions can be drawn:

- As the applied stress increases, there is a small reduction in the cross-sectional area of the sample.
- These results show that the elastic domain may not only avoid harming, but can sometimes enhance corrosion resistance, provided that the applied stress does not exceed a certain critical threshold.
- The observed corrosion rates all below 0.04 mm/year confirm that 316L stainless steel exhibits high resistance to uniform corrosion, even under elastic stress. This supports its suitability for use in aggressive environments.

## Scientific Ethics Declaration

\* The authors declare that the scientific ethical and legal responsibility of this article published in EPSTEM journal belongs to the authors.

## Conflict of Interest

\* The authors declare that they have no conflicts of interest

## Funding

\* This research received no specific grant from any funding agency in the public, commercial, or not-for-profit sectors.

## Acknowledgements or Notes

\* This article was presented as a poster presentation at the International Conference on Technology, Engineering and Science ([www.icontes.net](http://www.icontes.net)) held in Antalya/Türkiye on November 12-15, 2025.

\* The authors would like to thank the conference committee and EPSTEM journal reviewers for their valuable feedback

## References

Allou, D., Miroud, D., Ouadah, M., Cheniti, B., & Bouyagh, S. (2020). Criterion for cathodic protection of 25CD4/Inconel 182 system. *Applied Surface Science*, 502, 144100.

Allou, D. J., Ould Brahim, I., Cheniti, B., Fides, M., Hvizdos, P., Miroud, D. J., & Ziouche, A. (2021). Effect of post weld heat treatment on microstructure and mechanical behaviors of weld overlay Inconel 182 on 4130 steel substrate using SMAW process. *Metallography, Microstructure and Analysis*, 10(5), 567–578.

Benafia, S., Retraint, D., Yapi Brou, S., Panicaud, B., & Grosseau Poussard, J. L. (2018). Influence of surface mechanical attrition treatment on the oxidation behaviour of 316L stainless steel. *Corrosion Science*, 136, 188–200.

Cihal, V., & Ruscak, M. (1980). The influence of mechanical stress on the corrosion of metals. *Materials Science and Engineering*, 42, 1–15.

Djemmah, S., Madi, Y., Voué, M., Haddad, A., Allou, D., Ouallam, S., Bouchafaa, H., & Rezzoug, A. (2023). Effect of Mg addition on the morphology, roughness and adhesion of Cr chromized layer produced by pack cementation. *International Journal of Engineering, Transactions A: Basics*, 36, 1773–1782.

Djemmah, S., Voué, M., Madi, Y., Allou, D., Haddad, A., & Bouchafaa, H. (2024). Investigation of microstructural and electrochemical behavior of chromized-doped layers with variant magnesium concentrations. *Sādhanā*, 49(3), 243.

Frankel, G. S. (2003). *Electrochemical techniques in corrosion science and engineering*. CRC Press.

Krohn, H., & Virtanen, S. (2014). Effect of elastic and plastic deformation on the electrochemical behavior of austenitic stainless steels. *Corrosion Science*, 78, 186–191.

Liu, Y., Dai, H., Chen, S., He, M., Shi, S., Zhang, Z., & Chen, X. (2024). Study on stress corrosion behavior of 316L austenitic stainless steel in hot NaOH solution. *Journal of Materials Research and Technology*, 30, 8894–8905.

Macdonald, D. D. (2012). The history of the point defect model for the passive state. *Journal of The Electrochemical Society*, 159(6), C189–C217.

Marcus, P. (1998). Surface science approach of corrosion phenomena. *Electrochimica Acta*, 43(2–3), 109–118.

Marcus, P. (Ed.). (2011). *Corrosion mechanisms in theory and practice* (3rd ed.). CRC Press.

Ouadah, M., Touhami, O., Ibtiouen, R., Khorchef, M., & Allou, D. (2018). Corrosion effects on the magnetic behavior of magnetic circuit of an induction machine. *Progress in Electromagnetics Research M*, 68, 79–87.

Olsson, C.-O. A. (1995). Stainless steels for biomedical applications. *ISIJ International*, 35(1), 1–12.

Revie, R. W., & Uhlig, H. H. (2008). *Corrosion and corrosion control* (4th ed.). Wiley.

Sedriks, A. J. (1996). *Corrosion of stainless steels* (2nd ed.). Wiley-Interscience.

Tabor, D. (2000). *The hardness of metals*. Oxford University Press.

Wu, G., & Singh, P. M. (2019). Effect of elastic stresses on pitting behavior of stainless steel 304. *Journal of the Electrochemical Society*, 166(8).

Zhang, Y., Yang, C., Zhao, L., & Zhang, J. (2021). Study on the electrochemical corrosion behavior of 304 stainless steel in chloride ion solutions. *International Journal of Electrochemical Science*, 16, 210251.

---

### Author (s) Information

---

**Allou Djilali**

Research Center in Industrial Technologies (CRTI) Box 64,  
Cheraga, Algiers 16014, Algeria  
Contact e-mail: [djilallou@yahoo.fr](mailto:djilallou@yahoo.fr)

**Amraoui Rachid**

Research Center in Industrial Technologies (CRTI), P.O.  
Box 64, Chéraga, Algiers, Algeria.

**Djemmah Sarra**

University of Mons, Physics of Materials and Optics Unit  
(LPMO), Research Institute for Materials Science and  
Engineering Mons 7000, Belgium

**Benmohamed Manal**

Research Center in Industrial Technologies (CRTI), P.O.  
Box 64, Chéraga, Algiers, Algeria

**Younes Abderahman**

Research Center in Industrial Technologies (CRTI), P.O.  
Box 64, Chéraga, Algiers, Algeria

**Abada Abderahim**

Laboratory of Aeronautic Science, Aeronautic Institute,  
University of Saad Dahlab Blida 1, Algeria, Algeria

---

**To cite this article:**

Djilali, A., Rachid, A., Sarra, D., Manal, B., Abderahman, Y., & Abderahim, A. (2025). Effects of elastic deformation on the corrosion of 316L in 3.5% NaCl. *The Eurasia Proceedings of Science, Technology, Engineering and Mathematics*, 38, 316–322.